CHEMISTRY OF MATERIALS

COMMUNICATION

pubs.acs.org/cm

Low Temperature Growth of High Purity, Low Resistivity Copper Films by Atomic Layer Deposition

Thomas J. Knisley,[†] Thiloka C. Ariyasena,[†] Timo Sajavaara,[‡] Mark J. Saly,[§] and Charles H. Winter[*,†]

[†]Department of Chemistry, Wayne State University, Detroit, Michigan 48202, United States

[‡]Department of Physics, University of Jyväskylä, 40014 Jyväskylä, Finland,

[§]SAFC Hitech, 1429 Hilldale Avenue, Haverhill, Massachusetts 01832, United States

Supporting Information

KEYWORDS: copper, atomic layer deposition, thin films, precursor

Copper is the primary interconnect material in microelectronics devices, as a result of its low resistivity and high resistance to electromigration.[1] The dimensions of the smallest features in microelectronics devices are scheduled to reach 22 nm by 2012,[2] which places severe demands upon the film growth techniques used in device fabrication. The atomic layer deposition (ALD) film growth method is ideally suited for future microelectronics manufacturing, since it inherently provides highly conformal thin films, even in high aspect ratio nanoscale features, and allows subnanometer control over film thicknesses.[3] Copper metal needs to be deposited by ALD to meet future conformality and film thickness uniformity requirements in microelectronics devices. In addition, the copper metal should be deposited ideally at $\leq$100 °C to afford the smallest surface roughnesses, promote facile nucleation, and give continuous films, even at thicknesses of a few nanometers. Existing copper ALD processes have yet to meet all of these demands. Examples of direct copper ALD processes include $CuL_2/ZnEt_2$ at 100−150 °C (L = $OCHMeCH_2NMe_2$, β-ketiminate, β-diketiminate),[4,5] $Cu(thd)_2/H_2$ at 190−260 °C (thd = 2,2,6,6-tetramethyl-3,5-heptanedionate),[6] $[Cu(sBuNCMeNsBu)]_2/H_2$ at 150−250 °C,[7−9] $Cu(hfac)_2$/alcohol at 300 °C (hfac = 1,1,1,5,5,5-hexafluoro-3,5-pentanedionate),[10] $CuCl/H_2$ at 360−410 °C,[11] and CuCl/Zn at 440−500 °C.[12] The ALD growth of copper thin films was claimed from a copper(I) β-diketiminate precursor and diethylsilane,[13] but a later study showed that this process proceeds by a pulsed chemical vapor deposition (CVD) mechanism.[14] Indirect routes to copper films have included the reduction of ALD CuO by isopropanol,[15] the reduction of ALD Cu_3N with H_2,[16] and the reduction of ALD Cu_2O by formic acid in conjunction with a ruthenium seed layer.[17] Finally, plasma-based ALD processes include $Cu(acac)_2$/hydrogen plasma (acac = 2,4-pentanedionate)[18] and $Cu(OCHMeCH_2NMe_2)_2$/hydrogen plasma.[19] Problems with existing copper ALD processes include high growth temperatures, lack of self-limited growth in some of the systems, low reactivity of the copper precursors toward the reducing coreagents, incorporation of zinc in processes using $ZnEt_2$, and possible substrate damage and low conformal coverage in plasma processes.

Herein, we describe a new low temperature copper ALD process that employs a three precursor sequence entailing $Cu(OCHMeCH_2NMe_2)_2$ (**1**), formic acid, and hydrazine. In this process, **1** is unreactive toward hydrazine but is transformed to copper(II) formate, which is then readily reduced to copper metal by the hydrazine pulses. The present work therefore addresses a central problem with the ALD growth of metal thin films: low reactivity of the metal precursors toward common reducing coreagents. Analogous three-step processes comprising a metal precursor, a strong acid, and a reducing agent should allow the low temperature ALD growth of many transition metal thin films.

The growth of copper metal films by ALD was carried out using **1**, formic acid, and anhydrous hydrazine as precursors on Si(100) substrates with the native oxide. Precursor **1** has been previously reported[20,21] and is commercially available.[22] Initial ALD growth studies performed with **1** and formic acid at 120 °C afforded green-colored films that washed off of the substrate upon rinsing with deionized water. Presumably, this film corresponded to copper(II) formate, which is stable at the 120 °C deposition temperature. Thermogravimetric analysis (TGA) of copper(II) formate tetrahydrate revealed decomposition to copper metal starting at ∼225 °C, which is well above the decomposition temperature of **1**. Hence, copper film growth at $\geq$225 °C would proceed by a CVD-like mechanism as a result of the decomposition of **1**. It was previously reported that an aqueous solution of copper(II) formate undergoes rapid reduction to copper metal at ambient temperature upon treatment with hydrazine hydrate.[23] Accordingly, a three-step ALD process entailing **1**, formic acid, and hydrazine was examined. Precursor pulse lengths, substrate temperatures, and the number of cycles were varied to assess the growth behavior. The growth rate was investigated as a function of the pulse length of **1** at a substrate temperature of 120 °C. The number of deposition cycles, the lengths of the formic acid and hydrazine pulses, and the length of the purges after each pulse were kept constant at 1000, 0.2 s, 0.2 s, and 5.0 s, respectively. As shown in Figure 1a, pulse lengths for **1** of $\geq$3 s afforded a constant growth rate of about 0.50 Å/cycle. Similar experiments were used to explore the growth behavior as a function of the formic acid and hydrazine pulse lengths, using 1000 cycles, 3.0 s pulses of **1**, 5.0 s purges between precursor pulses, and a growth temperature of 120 °C. Plots of growth rate versus pulse length demonstrated saturative growth with formic

Received: August 19, 2011
Revised: September 19, 2011
Published: September 27, 2011

ACS Publications © 2011 American Chemical Society

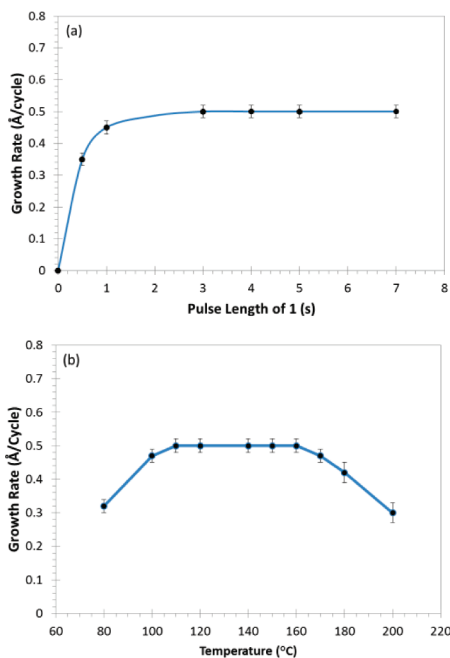

Figure 1. (a) Growth rate as a function of the pulse length of **1**. (b) Growth rate as a function of deposition temperature.

Table 1. Percentages of C, O, N, and H in Copper Films Obtained by TOF-ERDA

temp, °C	% C	% O	% N	% H
100	0.1 ± 0.1	0.5 ± 0.2	≤ 0.1	<0.5
120	1.0 ± 0.3	0.5 ± 0.2	0.2 ± 0.1	1.2 ± 0.5
140	0.5 ± 0.2	1.0 ± 0.3	0.15 ± 0.1	2.0 ± 0.5
160	0.9 ± 0.3	0.8 ± 0.3	0.15 ± 0.1	0.9 ± 0.4
180	1.2 ± 0.4	1.0 ± 0.3	0.4 ± 0.2	1.5 ± 0.5

acid and hydrazine pulse lengths of ≥ 0.1 s. These experiments demonstrate that the film growth at 120 °C proceeds by a self-limiting ALD growth mechanism. No copper metal film growth was observed at <200 °C with processes employing **1** and formic acid or **1** and hydrazine.

The growth rate as a function of deposition temperature was also investigated (Figure 1b). The conditions in these depositions consisted of pulse lengths of 3.0, 0.2, and 0.2 s for **1**, formic acid, and hydrazine, respectively, purge lengths of 5.0 s between pulses, and 1000 deposition cycles. A constant growth rate of 0.47−0.50 Å/cycle was observed between 100 and 170 °C (the ALD window). Lower growth rates occurred at 80, 180, and 200 °C.

The dependence of the film thickness on the number of deposition cycles was investigated next. In these experiments, the pulse lengths of **1**, formic acid, and hydrazine were 3.0, 0.2, and 0.2 s, respectively, with purge lengths of 5.0 s between pulses. The deposition temperature was 120 °C. The film thicknesses varied linearly with the number of cycles, and the slope of the line (0.50 Å/cycle) equaled the saturative growth rate established in Figure 1 (Figure S3 in the Supporting Information). The line of best fit shows a y-intercept of 1.46 nm, which is within the experimental error of zero and suggests efficient nucleation.

Time of flight elastic recoil detection analysis (TOF-ERDA) was performed on 45−50 nm thick films grown at 100, 120, 140, 160, and 180 °C to probe the elemental compositions (Table 1). The atomic compositions of the films ranged from 95.9 to 98.8% copper, 0.1−1.2% carbon, 0.5−1.0% oxygen, ≤ 0.4% nitrogen, and ≤ 2.0% hydrogen. In general, the films had the highest purity at 100 °C and the lowest purity at 180 °C. Growth at the latter temperature may include some precursor self-decomposition; however, the uncertainties in the compositions preclude more definitive conclusions. Simulations demonstrate that the majority of the impurities reside at the film surface and at the interface between copper and the silicon substrate. The carbon, oxygen, and hydrogen impurities may arise from postdeposition exposure to the ambient atmosphere or from traces of formate that remain in the film.

X-ray photoelectron spectroscopy (XPS) was performed on 50 nm thick copper films deposited at 140 °C to assess the composition of the films. The surface of the as-deposited film showed the expected ionizations arising from metallic copper, as well as small ionizations from oxygen and carbon. Nitrogen concentrations were at or below the detection limit (<1%). After argon ion sputtering, a constant composition of 95.1 wt % copper, 1.2 wt % carbon, 3.1 wt % oxygen, and <1 wt % nitrogen was observed. The Cu $2p_{1/2}$ and Cu $2p_{3/2}$ ionizations appeared at 952.2 and 932.4 eV, which are exact matches for copper metal.[24]

Powder X-ray diffraction experiments were performed on a 45 nm thick film deposited at 100 °C and on 50 nm thick films that were grown at 120, 140, 160, and 180 °C. All of the as-deposited films were crystalline and showed reflections arising from the (111), (200), and (220) planes of copper metal (JCPDS file no. 04-0836). The AFM image of a 50 nm thick film grown at 120 °C had a root mean square (rms) surface roughness of 3.5 nm. The SEM images of a film deposited under the same conditions showed no cracks or pinholes and a very uniform surface. The resistivities of 45−50 nm thick copper films deposited at 100, 120, and 140 °C ranged from 9.6 to 16.4 $\mu\Omega$ cm at 20 °C, compared to the bulk resistivity of copper of 1.72 $\mu\Omega$ cm at 20 °C. For comparison, sputtered 40−50 nm thick copper films on SiO_2 substrates had resistivities of 6−8 $\mu\Omega$ cm.[25] Hence, our resistivity values indicate high purity copper metal. Films grown at all temperatures passed the Scotch tape test, demonstrating good adhesion.

The best previous low temperature copper ALD process, entailing **1** and $ZnEt_2$, is reported to afford high purity copper films within the 100−120 °C ALD window.[4] However, a subsequent report documented a parasitic chemical vapor deposition (CVD) reaction of $ZnEt_2$ that leads to Zn incorporation into the copper films at temperatures between 120 and 150 °C.[5] In the latter study, the copper(II) pyrrolylaldiminate precursor had a minimum deposition temperature of 120 °C, but zinc is likely deposited even at 100−120 °C in processes that employ $ZnEt_2$. The process described herein avoids undesired elements in the precursors, and affords high purity, low resistivity copper metal at all growth temperatures that were examined. Formic acid (pK_a = 3.7[26]) is strongly acidic and should lead to very favorable protonation equilibria of the ligands in nearly all classes of commonly used metal precursors. Hence, the treatment of a surface-bound metal precursor with formic acid should lead to rapid and efficient ligand removal and formation of a surface-bound metal formate. Formic acid has been previously employed in ALD to reduce Cu_2O films to copper metal,[17] but a ruthenium seed layer was required to catalyze the elimination of carbon dioxide from the surface formate species. The use of formic acid as a coreagent in the CVD growth of copper metal films was demonstrated,[27]

but the films were deposited on ruthenium substrates that likely catalyze the decomposition of the surface formates. Preliminary experiments using acetic acid in place of formic acid also afforded copper metal with **1** and hydrazine, which implies that a range of other protic acids can be employed. If the film growth temperature is below the thermal decomposition point of the metal formate, then a subsequent hydrazine pulse leads to the reduction to the metal, as exemplified by copper metal growth in the present work. Presumably, reducing coreagents other than hydrazine can also be used. Metals such as ruthenium that can catalyze the low temperature elimination of carbon dioxide from formates may not require a reducing precursor. Preliminary results demonstrate that an analogous process entailing $Ni(OCHMeCH_2NMe_2)_2$, formic acid, and hydrazine leads to nickel metal thin films at a substrate temperature of 175 °C. The reduction of the nickel(II) ion to nickel metal occurs at $E° = -0.25$ V,[28] which implies that the low temperature ALD growth of other metal films may be achieved with a metal precursor, a strong acid, and an optional reducing reagent (as noted above) for metal ions with electrochemical potentials greater than that of the nickel(II) ion. Metal ions in this category include silver, gold, palladium, platinum, rhodium, iridium, rhenium, tungsten, and others.[28] The ALD growth of many of these metals is well documented, but thermal ALD usually occurs at >200 °C to provide enough activation energy to drive the ligand combustion reactions that occur with the oxygen coreagent.[29,30]

■ ASSOCIATED CONTENT

Ⓢ Supporting Information. Experimental procedures and film characterization data (pdf). This material is available free of charge via the Internet at http://pubs.acs.org.

■ AUTHOR INFORMATION

Corresponding Author
*E-mail: chw@chem.wayne.edu.

■ ACKNOWLEDGMENT

This work was supported by the U.S. National Science Foundation (Grant No. CHE-0910475) and SAFC Hitech.

■ REFERENCES

(1) Kim, H. *Surf. Coat. Technol.* **2006**, *200*, 3104–3111.
(2) International Technology Roadmap for Semiconductors, http://www.itrs.net/.
(3) Leskelä, M.; Ritala, M. *Angew. Chem., Int. Ed.* **2003**, *42*, 5548–5554.
(4) Lee, B. H.; Hwang, J. K.; Nam, J. W.; Lee, S. U.; Kim, J. T.; Koo, S.-M.; Baunemann, A.; Fischer, R. A.; Sung, M. M. *Angew. Chem., Int. Ed.* **2009**, *48*, 4536–4539.
(5) Vidjayacoumar, B.; Emslie, D. J. H.; Clendenning, S. B.; Blackwell, J. M.; Britten, J. F.; Rheingold, A. *Chem. Mater.* **2010**, *22*, 4844–4853.
(6) Hsu, I. J.; McCandless, B. E.; Weiland, C.; Willis, B. G. *J. Vac. Sci. Technol., A* **2009**, *27*, 660–667.
(7) Lim, B. S.; Rahtu, A.; Gordon, R. G. *Nat. Mater.* **2003**, *2*, 748–754.
(8) Li, Z.; Rahtu, A.; Gordon, R. G. *J. Electrochem. Soc.* **2006**, *153*, C787-C794.
(9) Li, Z.; Gordon, R. G.; Farmer, D. B.; Lin, Y.; Vlassak, J. *Electrochem. Solid-State Lett.* **2005**, *8*, G182–G185.
(10) Solanki, R.; Pathangey, B. *Electrochem. Solid-State Lett.* **2000**, *3*, 479–480.
(11) Mårtensson, P.; Carlsson, J.-O. *Chem. Vap. Deposition* **1997**, *3*, 45–50.
(12) Juppo, M.; Ritala, M.; Leskelä, M. *J. Vac. Sci. Technol., A* **1997**, *15*, 2330–2333.
(13) Park, K.-H.; Bradley, A. Z.; Thompson, J. S.; Marshall, W. J. *Inorg. Chem.* **2006**, *45*, 8480–8482.
(14) Thompson, J. S.; Zhang, L.; Wyre, J. P.; Brill, D. J.; Lloyd, K. G. *Thin Solid Films* **2009**, *517*, 2845–2850.
(15) Huo, J.; Solanki, R. *J. Mater. Res.* **2002**, *17*, 2394–2398.
(16) Li, Z.; Gordon, R. G. *Chem. Vap. Deposition* **2006**, *12*, 435–441.
(17) Waechtler, T.; Ding, S.-F.; Hofmann, L.; Mothes, R.; Xie, Q.; Oswald, S.; Detavernier, C.; Schulz, S. E.; Qu, X.-P.; Lang, H.; Gessner, T. *Microelectron. Eng.* **2011**, *88*, 684–689.
(18) Niskanen, A.; Rahtu, A.; Sajavaara, T.; Arstila, K.; Ritala, M.; Leskelä, M. *J. Electrochem. Soc.* **2005**, *152*, G25–G28.
(19) Moon, D.-Y.; Han, D.-S.; Shin, S.-Y.; Park, J.-W.; Kim, B. M.; Kim, J. H. *Thin Solid Films* **2011**, *519*, 3636–3640.
(20) Goel, S. C.; Kramer, K. S.; Chiang, M. Y.; Buhro, W. E. *Polyhedron* **1990**, *9*, 611–613.
(21) Becker, R.; Devi, A.; Weiss, J.; Weckenmann, U.; Winter, M.; Kiener, C.; Becker, H.-W.; Fischer, R. A. *Chem. Vap. Deposition* **2003**, *9*, 149–156.
(22) We determined that **1** has a melting point of 139−141 °C, sublimes on a preparative scale (∼ 1 g) at 90 °C/0.05 Torr in ∼ 4 h with 89% sublimed recovery and 3% nonvolatile residue, and undergoes solid state thermal decomposition between 185 and 188 °C.
(23) Ravindranathan, P.; Patil, K. C. *Thermochim. Acta* **1983**, *71*, 53–57.
(24) *Handbook of X-ray Photoelectron Spectroscopy*; Wagner, C. D., Riggs, W. M., Davis, L. E., Moulder, J. F., Murlenberg, G. E., Eds.; Perkin-Elmer Corporation: Eden Prairie, MN; 1979, pp 81, 82.
(25) Barnat, E. V.; Nagakura, D.; Wang, P.-I.; Lu, T.-M. *J. Appl. Phys.* **2002**, *91*, 1667–1672.
(26) *CRC Handbook of Chemistry and Physics*, 91st ed.; Haynes, W. M., Ed.; CRC Press: 2010−2011; pp 8-20, 8-29.
(27) Song, H.; Norman, J. A. T.; Shimogaki, Y. *Microelectronics Eng.* **2010**, *87*, 249–253.
(28) *CRC Handbook of Chemistry and Physics*; 91st ed.; Haynes, W. M., Ed.; CRC Press: 2010−2011; pp 8−45.
(29) Aaltonen, T.; Ritala, M.; Tung, Y.-L.; Chi, Y.; Arstila, K.; Meinander, K.; Leskelä, M. *J. Mater. Res.* **2004**, *19*, 3353–3358.
(30) Knapas, K.; Ritala, M. *Chem. Mater.* **2011**, *23*, 2766–2771.